

Autofluorescence insensitive imaging using upconverting nanocrystals in scattering media

Can T. Xu,^{1,a)} Niclas Svensson,¹ Johan Axelsson,¹ Pontus Svenmarker,¹ Gabriel Somesfalean,¹ Guanying Chen,² Huijuan Liang,² Haichun Liu,² Zhiguo Zhang,² and Stefan Andersson-Engels¹

¹Department of Physics, Lund University, P.O. Box 118, S-221 00 Lund, Sweden

²Department of Physics, Harbin Institute of Technology, P.O. Box 3025, Harbin 150080, People's Republic of China

(Received 27 August 2008; accepted 1 October 2008; published online 27 October 2008)

Autofluorescence is a nuisance in the field of fluorescence imaging and tomography of exogenous molecular markers in tissue, degrading the quality of the collected data. In this letter, we report autofluorescence insensitive imaging using highly efficient upconverting nanocrystals ($\text{NaYF}_4:\text{Yb}^{3+}/\text{Tm}^{3+}$) in a tissue phantom illuminated with near-infrared radiation of 85 mW/cm^2 . It was found that imaging with such nanocrystals leads to an exceptionally high contrast compared to traditional downconverting fluorophores due to the absence of autofluorescence. Upconverting nanocrystals may be envisaged as important biological markers for tissue imaging purposes. © 2008 American Institute of Physics. [DOI: 10.1063/1.3005588]

In recent years, the interest for fluorescence diffuse optical imaging and tomography has grown tremendously.¹⁻³ Much of the work has been focused on developing inexpensive and compact systems for macroscopic imaging of fluorophores embedded in small animals. The systems could, for example, be used to monitor the effects from drugs on cancer tumors over a period of time, without sacrificing the animals. Extensive research has been performed both on the practical and the theoretical side in this area. Currently, mainly traditional dyes are used as fluorophores. These dyes emit Stoke shifted light upon excitation, and can be very effective with quantum efficiencies close to unity. However, since tissue itself autofluoresces due to several endogenous fluorophores mainly in the skin, a background fluorescence from the bulk tissue will always exist.^{4,5} In the presence of tissue autofluorescence, different spectral unmixing algorithms can also be used to extract the signal. These algorithms utilize the spectral characteristics of the fluorophores and the autofluorescence.⁶ However, the measurement procedure can be quite complex since one needs to acquire the emission at multiple wavelengths. To suppress the effects of autofluorescence, several approaches have been suggested. The two most promising ones are based on quantum dots and upconverting markers.

Quantum dots have been used as fluorophores in a great number of studies.⁷⁻⁹ Their large Stoke shift and narrow emission spectra allow the emission to be detected in a spectral band with low tissue autofluorescence. Quantum dots are very bright fluorophores due to their high absorption, mainly in the UV region. Their emission wavelength is dependent on the core size and can be selected over a wide range while the same excitation wavelength can be used.⁷ The main drawback at this stage for these fluorophores is their toxicity, together with the fact that penetration of the UV light is low in tissue. Typical quantum dots are based on CdSe due to the well established fabrication technology.¹⁰ Recent studies have shown that these quantum dots are potentially harmful

to organisms.^{11,10} The quantum dots tend to destabilize when exposed to biological environments. Adding the fact that they can easily penetrate into cells, the damage can be quite substantial. Research, however, is underway to produce less harmful quantum dots, as well as enhancing their biocompatibility.¹²

Upconverting nanoparticles have been proposed as a fluorophore in biomedical imaging applications due to their unique property to efficiently emit anti-Stoke shifted light upon near-infrared excitation.^{13,14} The main challenge has been to develop upconverting markers with high-quantum yield in the wavelength region above 650 nm where tissue is relatively transparent.

In this letter, we demonstrate autofluorescence insensitive imaging with novel high-quantum yield upconverting nanoparticles emitting at 800 nm. The study is performed in a controlled environment within tissue phantoms in which autofluorescence is simulated, and comparison with ordinary Stoke shifted fluorophores emitting at the same wavelength is made.

Efficient upconverting phosphors of nanometer size have been fabricated.¹⁴ The particles are doped with Yb^{3+} , which acts as sensitizer, and another rare earth ion, which acts as activator.¹⁵ By using different activators, various emission wavelengths can be accomplished with the same excitation wavelength. It has been shown that NaYF_4 is the most efficient host known for upconverting phosphorous crystals.¹⁶ In this study, highly efficient NaYF_4 crystals doped with Yb^{3+} and Tm^{3+} were used, which were prepared according to the procedure described in detail in Ref. 17. The particles absorb light at 980 nm and emit upconverted light at 800 nm. The process involves absorption of two or more photons with an intermediate metastable state.¹⁵ Figure 1 shows the emission spectrum for the nanoparticles, the blue emission line at 477 nm is only visible for higher pump intensities. The pump-power dependence of the 800 nm line was measured to be quadratic (slope=2.0) using low intensities, as seen in the inset of Fig. 1, suggesting a two-photon process.

^{a)}Electronic mail: can.xu@fysik.lth.se.

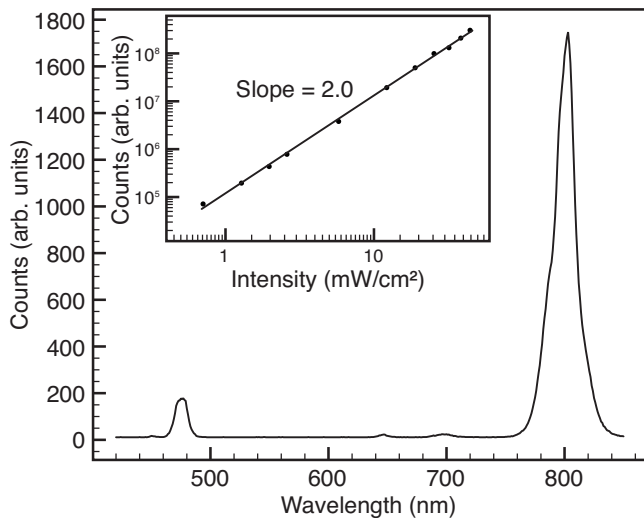


FIG. 1. Emission spectrum recorded for the nanoparticles under 980 nm excitation with an intensity of 6 W/cm². The inset shows the pump-power dependence of the interesting 800 nm line measured under low intensities.

A tissue phantom consisting of water, intralipid, and ink was prepared. The optical properties of the tissue phantom were measured with a time-of-flight spectroscopy system,¹⁸ and determined to have a reduced scattering coefficient $\mu'_s = 6.5 \text{ cm}^{-1}$ and an absorption coefficient $\mu_a = 0.44 \text{ cm}^{-1}$ for $\lambda = 660 \text{ nm}$. The parameters were chosen to have a good correspondence to real tissue in small animals.¹⁹ Two capillary tubes with inner diameters of 2.4 mm were used as containers for the fluorophores.

The imaging system is schematically shown in Fig. 2. The tubes were submerged into the tissue phantom to a depth of 5.0 mm, where the depth was taken as the distance from the front surface of the tubes to the surface of the phantom. Fiber-coupled lasers were used to illuminate the phantom with a slightly divergent beam. The spot sizes of the lasers on the phantom were approximately 1 cm². An air cooled charge coupled device (CCD) camera captured the images through a set of dielectric bandpass filters centered at 800 nm.

The first tube was filled with a solution of the nanocrystals dissolved in dimethyl sulfoxide (DMSO) with a concentration of 1 wt %. To excite the nanoparticles, a 978 nm laser diode was used, with a power of approximately 85 mW on

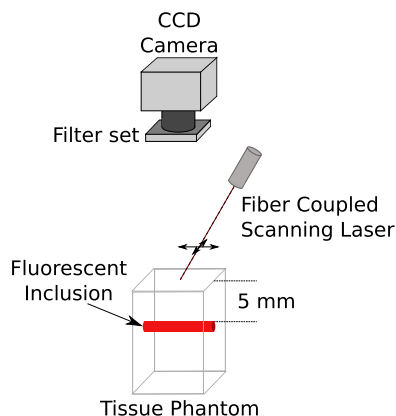


FIG. 2. (Color online) Schematic of the imaging setup. Light from a fiber-coupled laser is scanned in an array on the surface of the phantom. An air cooled CCD camera is used to capture an image for every scanned position.

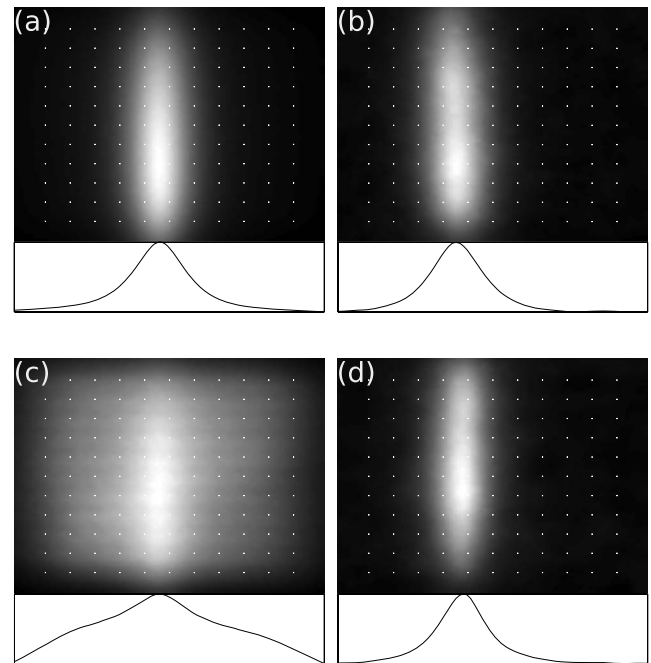


FIG. 3. Images comparing the DY-781 dye and the nanoparticles with and without autofluorescence, along with plots showing the sums in the vertical directions. The white dots have been added artificially and represent the positions used for the excitation light. The left column shows the results using DY-781, and the right column shows the results using upconverting nanoparticles. (a) and (b) are taken without any added autofluorophores. (c) and (d) are taken with a background autofluorophore concentration of 40 nM.

the surface of the tissue phantom. The second tube was filled with a solution of ordinary fluorophores (DY-781, Dyomics GmbH) dissolved in ethanol with a concentration of 1 μM . The fluorophores were excited with a 780 nm laser diode with a power of 40 mW on the surface of the phantom. The concentration of the nanoparticles is reasonably consistent with studies performed using quantum dots *in vivo*. In those studies, approximately 1 nmol of CdSe quantum dots were injected into a mouse ($\sim 18 \text{ g}$), giving an approximate concentration of 0.01 wt % if distributed homogeneously.^{8,9} With functionalized quantum dots, selective accumulation in tumors can be achieved. Taking this into consideration and the fact that the nanoparticles have molar mass of the same order of magnitude as the quantum dots, the concentration of 1 wt % used in this study seems acceptable.

The lasers were raster scanned in a $4.4 \times 4.4 \text{ cm}^2$ array consisting of 121 positions, and an image was acquired for every laser position. In order to minimize the effects of random bright pixels, a median filter with a mask of 3×3 pixels was applied to all images. The individual images were then summed, and a representation of the photon distribution on the surface was obtained. Even if this does not accurately reflect the fluorophore distribution, it enables detection of fluorescent inclusions. To mimic tissue autofluorescence, a small amount of DY-781 was also added into the phantom.

Figure 3 shows images taken with and without autofluorescence. As expected, the autofluorescence effectively hides the signal from the inclusion with the ordinary fluorophores [Fig. 3(c)], while no background appears on the images using the upconversion scheme [Fig. 3(d)]. It is worth to notice that using traditional fluorophores, even without any artificial

autofluorophores added, the autofluorescence introduced by the intralipid within the phantom is visible, see the cross section profile in Fig. 3(a).

As seen in Fig. 3, the signal-to-background contrast is superior for upconverting nanoparticles emitting in a wavelength region where no Stoke shifted tissue autofluorescence is present. Higher excitation power can increase the signal-to-noise ratio, without sacrificing the high contrast. Increasing the signal-to-noise ratio, however, will not boost the image quality using traditional fluorophores since they are limited by a lower signal-to-background contrast due to the ubiquitous autofluorescence. Even with the lower quantum efficiency of the nanoparticles compared to traditional fluorophores the image quality is therefore expected to be better.

Background caused by autofluorescence is very prominent when working with an epifluorescence imaging setup in comparison to a fluorescence transmission imaging setup. In the latter setup, it is possible to suppress the autofluorescence signal fairly effectively.²⁰ However, such a system can be very ineffective when used to detect and image a superficial signal.

The particles used for this study were still in the development stage. For example, they were in bulk state without any kind of coating, and thus not soluble in water and therefore not biocompatible. However, improved fabrication methods can make them water soluble.^{21,22} In addition, there are also reports suggesting that coating the particles with an undoped layer reduces the nonradiative losses at the surface, thus effectively enhancing their upconversion efficiency.^{22,23} Using a pulsed light source with a higher peak power should further increase the signal tremendously, due to the quadratic pump-power dependence of the upconverting process. Such a light source should still be harmless in terms of tissue heating and damaging, since the mean power can still be kept low.

Future work will involve the use of nanocrystals for diffuse optical tomography. With their unique features in emitting a signal that is insensitive to the downconverting autofluorescence, they have the potential to become an important biological marker. In a longer perspective we hope to functionalize the particles with tumor seeking properties. Early studies by other groups have already been performed, and the prospects are very promising.²⁴

We gratefully acknowledge Erik Alerstam and Tomas Svensson for their assistance with the time-of-flight measurements. This work was supported by the EC integrated projects Molecular Imaging LSHG-CT-2003-503259 and Brighter 1ST-2005-035266, as well as by VR-SIDA 348-2007-6939.

- ¹V. Ntziachristos, *Annu. Rev. Biomed. Eng.* **8**, 1 (2006).
- ²V. Ntziachristos, J. Ripoll, L. Wang, and R. Weissleder, *Nat. Biotechnol.* **23**, 313 (2005).
- ³L. Sampath, W. Wang, and E. M. Sevick-Muraca, *J. Biomed. Opt.* **13**, 041312 (2008).
- ⁴G. Wagnieres, W. Star, and B. Wilson, *Photochem. Photobiol.* **68**, 603 (1998).
- ⁵S. Andersson-Engels and B. Wilson, *J. Cell Pharmacol.* **3**, 48 (1992).
- ⁶D. Farkas, C. Du, G. Fisher, C. Lau, W. Niu, E. Wachman, and R. Levenson, *Comput. Med. Imaging Graph.* **22**, 89 (1998).
- ⁷M. Bruchez, M. Moronne, P. Gin, S. Weiss, and A. Alivisatos, *Science* **281**, 2013 (1998).
- ⁸X. Gao, Y. Cui, R. M. Levenson, L. W. K. Chung, and S. Nie, *Nat. Biotechnol.* **22**, 969 (2004).
- ⁹B. Ballou, B. Lagerholm, L. Ernst, M. Bruchez, and A. Waggoner, *Bioconjugate Chem.* **15**, 79 (2004).
- ¹⁰V. Karabanovas, E. Zakarevicius, A. Sukackaitė, G. Streckyte, and R. Rotomskis, *Photochem. Photobiol. Sci.* **7**, 725 (2008).
- ¹¹A. O. Choi, S. E. Brown, M. Szyf, and D. Maysinger, *J. Mol. Med.* **86**, 291 (2008).
- ¹²W. B. Cai, A. R. Hsu, Z. B. Li, and X. Y. Chen, *Nanoscale Res. Lett.* **2**, 265 (2007).
- ¹³J. Shan and Y. Ju, *Appl. Phys. Lett.* **91**, 123103 (2007).
- ¹⁴S. Heer, K. Kompe, H. Güdel, and M. Haase, *Adv. Mater. (Weinheim, Ger.)* **16**, 2102 (2004).
- ¹⁵F. Auzel, *Chem. Rev. (Washington, D.C.)* **104**, 139 (2004).
- ¹⁶K. Kramer, D. Biner, G. Frei, H. Güdel, M. Hehlen, and S. Luthi, *Nano Lett.* **4**, 2191 (2004).
- ¹⁷G. Yi, H. Lu, S. Zhao, Y. Ge, W. Yang, D. Chen, and L.-H. Guo, *Nano Lett.* **4**, 2191 (2004).
- ¹⁸E. Alerstam, S. Andersson-Engels, and T. Svensson, *J. Biomed. Opt.* **13**, 041304 (2008).
- ¹⁹V. Ntziachristos, E. Schellenberger, J. Ripoll, D. Yessayan, E. Graves, A. Bogdanov, L. Josephson, and R. Weissleder, *Proc. Natl. Acad. Sci. U.S.A.* **101**, 12294 (2004).
- ²⁰G. Zacharakis, H. Shih, J. Ripoll, R. Weissleder, and V. Ntziachristos, *Mol. Imaging* **5**, 153 (2006).
- ²¹F. Wang, D. K. Chatterjee, Z. Li, Y. Zhang, X. Fan, and M. Wang, *Nanotechnology* **17**, 5786 (2006).
- ²²G.-S. Yi and G.-M. Chow, *Chem. Mater.* **19**, 341 (2007).
- ²³J. Suyver, A. Aebischer, D. Biner, P. Gerner, J. Grimm, S. Heer, K. Kramer, C. Reinhard, and H. Güdel, *Opt. Mater. (Amsterdam, Neth.)* **27**, 1111 (2005).
- ²⁴Q. Lü, F. Guo, L. Sun, A. Li, and L. Zhao, *J. Phys. Chem. C* **112**, 2836 (2008).